Published in Nuclear Fusion **47** (2007) 1607

The Deuterium Inventory in ASDEX Upgrade

M. Mayer[1], V. Rohde[1], G Ramos[2], E. Vainonen-Ahlgren[3], J. Likonen[3], A. Herrmann[1], R. Neu[1], and ASDEX Upgrade Team

[1] Max-Planck-Institut für Plasmaphysik, EURATOM Association, Boltzmannstr. 2, D-85748 Garching, Germany

[2] CICATA-Qro, Instituto Politécnico Nacional, José Siurob 10, Col. Alameda, 76040 Querétaro, México

[3] VTT, Association EURATOM-Tekes, P.O. Box 1000, 02044 VTT, Finland

E-mail: Matej.Mayer@ipp.mpg.de

Abstract. The deuterium inventory in ASDEX Upgrade was determined by quantitative ion beam analysis techniques and SIMS for different discharge campaigns between the years 2002 and 2005. ASDEX Upgrade was a carbon dominated machine during this phase. Full poloidal sections of the lower and upper divertor tile surfaces, limiter tiles, gaps between divertor tiles, gaps between inner heat shield tiles, and samples from remote areas below the roof baffle and in pump ducts were analyzed, thus offering an exhaustive survey of all relevant areas in ASDEX Upgrade. Deuterium is mainly trapped on plasma exposed surfaces of inner divertor tiles, where about 70% of the retained deuterium inventory are found. About 20% of the inventory are retained at or below the divertor roof baffle, and about 10% are observed in other areas, such as the outer divertor and in gaps between tiles. The long term deuterium retention is 3–4% of the total deuterium input. The obtained results are compared to gas balance measurements, and conclusions about tritium retention in ITER are made.

PACS numbers: 52.40.Hf; 52.55.Fa; 28.52.Fa; 52.55.Rk; 82.80.Yc

1. Introduction

Major disadvantages of carbon as plasma facing material are its high chemical erosion yield under hydrogen bombardment [1, 2], and its ability to trap large amounts of hydrogen by codeposition [3]. This may result in unacceptably high tritium inventories in ITER [4, 5].

Predictions of the expected tritium inventory in ITER are based on modelling calculations of global carbon erosion, transport and co-deposition. However, these predictions are subject to large uncertainties due to inaccuracies of basic input data (such as erosion yields, sticking coefficients, hydrogen inventories in mixed materials, etc.) and lack of understanding of the basic physics of plasma flows and material transport. Today's machines allow the different mechanisms of carbon transport to

be investigated, and they allow the accuracy of models used for predictions for ITER to be checked.

This paper presents an extensive survey of the deuterium inventory trapped in different wall areas during the carbon dominated phase of ASDEX Upgrade. The work comprises investigations of lower and upper divertor tiles, limiter tiles, gaps between tiles, and different remote areas. The data obtained from post-mortem surface analysis are compared to gas balance data.

2. Experimental

2.1. Wall materials

ASDEX Upgrade started the replacement of carbon tiles by tungsten coated ones in summer 1999, aiming at a full tungsten machine in the year 2007 [6]. A cross-section of the machine is shown in Fig. 1, the lower divertor is shown in more detail in Fig. 2. The inner divertor is formed by tiles 4, 5, 6A and 6B. Tiles 9A, 9B and 9C are the roof baffle, and tiles 10, 1, 2 and 3 the outer divertor. Tiles 1, split into 1A and 1B, are the outer, and tile 4 the inner strike point tiles. All tiles consist of fine grain graphite manufactured by Ringsdorff or Schunk, only tile 4 is made from carbon-fibre composite (CFC), type N11 from SEP. Tiles 6A and 6B were coated with W using physical vapor deposition (PVD) in summer 2002, tiles 2, 3A and 3B were coated with W in summer 2004, and roof baffle tiles 9A, 9B and 9C followed in summer 2005.

The main chamber was fully covered with carbon tiles until 1999. The replacement of carbon inner heat shield tiles by tungsten coated ones started in 1999, and the inner heat shield was already fully coated with tungsten during the 2002–2003 campaign. All upper divertor tiles and the protection tiles of the upper passive stabilizer loop (PSL) were coated with tungsten in summer 2003. The lower PSL protection tiles were replaced by W-coated ones in summer 2005.

Four ICRH antennae protection limiter frames and four auxiliary limiters in the main chamber were initially made from carbon. The carbon tiles were successively replaced by tungsten coated ones in summer 2004 and summer 2005.

2.2. Plasma operation

The 2002–2003 campaign lasted from 11/2002 to 8/2003. 1237 plasma discharges with 4856 s plasma in lower divertor configuration were performed during this discharge period. Six boronizations and one siliconization were applied for wall conditioning. The discharge period 2003–2004 lasted from 12/2003 to 08/2004. 1284 discharges with a total plasma time of 4131 s were performed, of which 3733 s were with X-point in lower divertor configuration and 232 s in upper divertor configuration. Eight boronizations were applied. The discharge period 2004–2005 lasted from 11/2004 to 07/2005. 1099 plasma discharges with a total plasma time of 3864 s, of which 3057 s were plasma in lower divertor configuration, were performed. Six boronizations were applied.

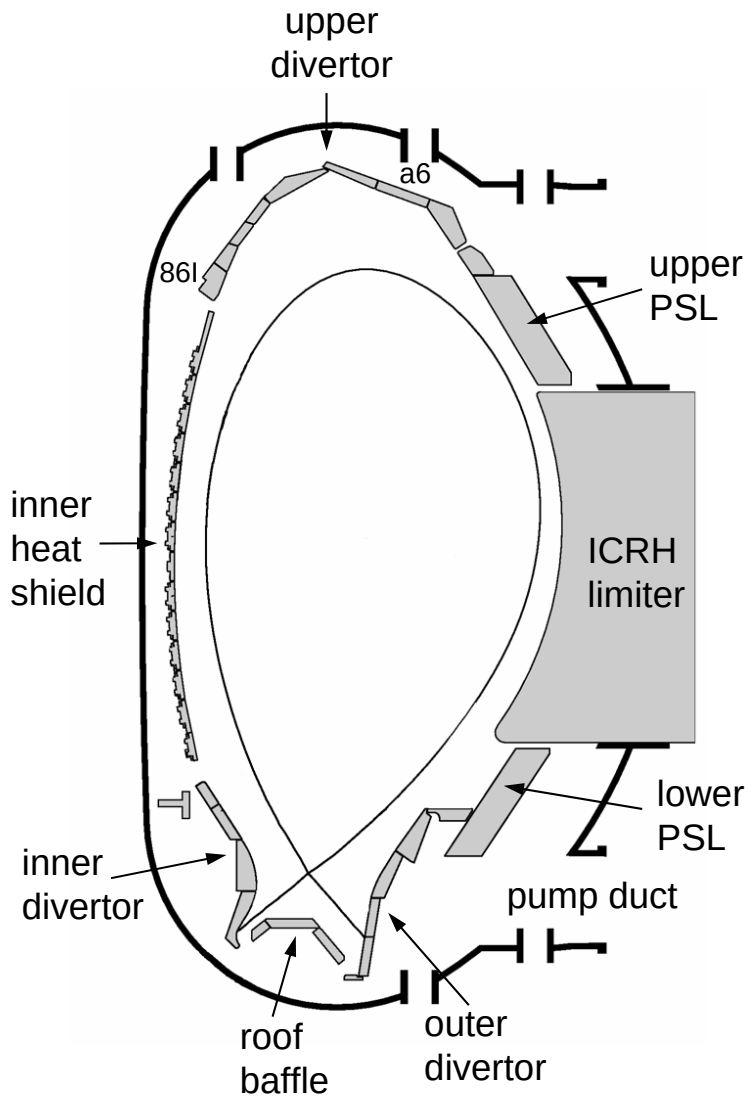

Figure 1. ASDEX Upgrade with divertor IIb. PSL is the passive stabilizer loop. Some tile numbers for the upper divertor are indicated. See Fig. 2 for details of the lower divertor.

2.3. Analyzed samples

In order to determine erosion and deposition of carbon in the divertor during the 2002–2003 campaign [7], a poloidal section of tiles from sector 11 was coated with a marker consisting of 1.6×10^{18} Re-atoms/cm^2 (about 230 nm), and 3.1×10^{19} (about 3.1 μm‡) carbon on top using a pulsed plasma arc [8]. The marker layer width was 15 mm. The Re serves as marker for ion beam analysis and secondary ion mass spectrometry (SIMS), thus allowing the thickness of the overlaying carbon layer to be measured. Another set consisting of divertor tiles 6A, 6B, 5, 10, 1, 2, 3A and 3B was used during the 2004–2005 campaign [9]. The tiles contained a Re/C marker stripe comparable to the

‡ For simplicity we use a carbon density of 1×10^{23} at/cm^3 = 2 g/cm^3 throughout this paper.

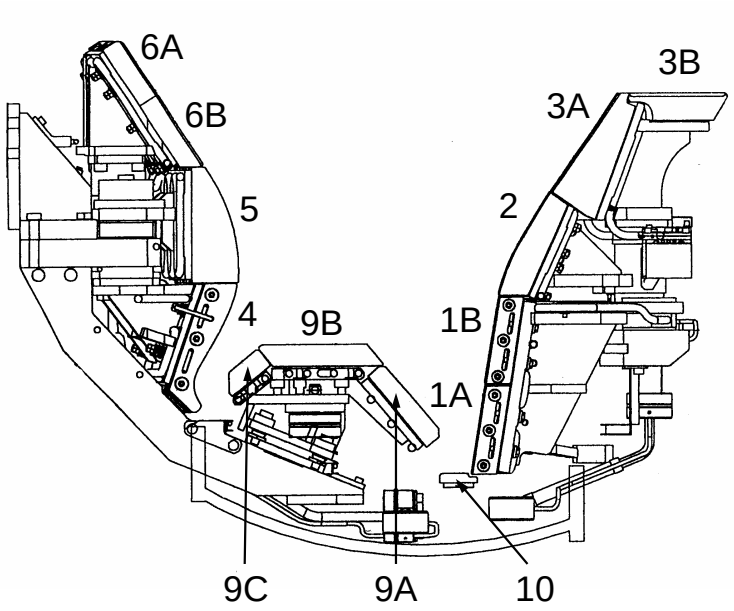

Figure 2. Layout of ASDEX Upgrade divertor IIb, as used during the period of the investigations. Numbers indicate tile numbers, as used throughout this paper.

2002–2003 tiles, and in addition a tungsten marker stripe [9]. For the sake of better readability we use the tile numbers as shown in Fig. 2 throughout this paper. This is a simplification of the full ASDEX Upgrade tile numbering scheme. The following tiles were used: 1A : 1b/24/34; 1B : 1b/17/09; 2 : 2b/4; 3A : 3b/4; 3B : 3/7; 4 : 4/2; 5 : 5/4; 6A : 6b/1-1; 6B : 6b/1-2; 9A : 9b/7; 9B : 9b/5; 9C : 9b/3; 10 : 10b/2.

35 long-term samples (LTS) were installed during the 2002–2003 campaign below the roof baffle and in remote areas in order to measure the carbon and deuterium co-deposition [10, 11]. A full poloidal section of upper divertor tiles consisting of 7 tiles was installed during the 2003–2004 campaign. Upper PSL protection tiles from this campaign were also analyzed. Three tiles (numbers 1, 4, 8) from the auxiliary limiter in segment 16/1 and one tile (number 2) from the limiter in segment 14/15 were analyzed after the 2005/2006 campaign.

Analyses of the deuterium inventory were always performed on an uncoated part of the graphite tiles. Fresh tiles were installed before the start of the discharge campaign and removed at the end.

2.4. Analysis methods

Marker layers on divertor or limiter tiles were analyzed prior to installation with Rutherford-backscattering (RBS) using 1.6 MeV protons at a scattering angle of 165°. The coatings were typically homogeneous with a thickness variation of less than 5% on most tiles. The tiles were analyzed again after exposure using RBS under the same conditions. For thicker layers 2.5 MeV protons were used. The information depth is about 13 μm for 1.6 MeV protons, and about 26 μm at 2.5 MeV. The spectra were

evaluated with the program SIMNRA [12, 13, 14] using non-Rutherford cross-section data from [15, 16, 17].

Deuterium was detected by nuclear reaction analysis (NRA) using the $D(^3He,p)^4He$ reaction at 0.8, 1.0 and 2.5 MeV incident energy, having information depths of 1.3, 2 and 10 μm§. Deuterium measurements were always made on uncoated tiles about 10 mm away from the marker stripes. Due to inaccuracies of the target current measurement on large tiles, an a-C:D target with known amount of D (1.5×10^{18} D-atoms/cm^2) was used for absolute calibration. The energy dependence of the nuclear reaction cross-section [18] plays a role for layer thicknesses above about 1 μm and was taken into account assuming a homogeneous layer composition. This introduces an error below 10% for inhomogeneous layers with depth-dependent deuterium concentrations, as are actually observed on the tiles. The accuracy of the determination of the amount of D is about 20%, mainly due to the inaccuracy of the target current measurement.

Secondary ion mass spectrometry (SIMS) measurements were performed using a scanned beam of 5 keV O_2^+ [19]. The depth calibration was obtained by measuring the SIMS crater depth with a profiler. The secondary ion yields of D and C are influenced by the concentration of boron: An increase of the boron concentration increases the ion yields of other elements. This matrix effect is taken into account by using the $D/^{12}C$ signal ratio, which is (almost) insensitive to the boron concentration.

The amount of C deposited on the long-term samples (LTS) was determined with RBS using 1.5 MeV protons and by NRA using the $^{12}C(^3He,p_1)^{14}N$ nuclear reaction at 2.5 MeV incident energy. D was detected using the $D(^3He,p)^4He$ reaction at 0.8 and 2.5 MeV energy [18].

3. Results

3.1. Divertor tiles

The distribution of strike point positions during the discharge campaign 2002–2003 is shown in Fig. 3(top). The s-coordinate, which is used for the figure, starts at the upper corner of tile 6A and follows the tile surfaces. The inner strike point was mostly on tile 4, and only a few discharges had the strike point on the roof baffle tile 9B. The outer strike point was always on tiles 1A or 1B.

The deposition of boron and carbon is shown in Fig. 3(middle), a magnified view of the inner divertor is shown in Fig. 4(top left). The whole inner divertor is a net deposition area, and thick deposits are observed on tiles 6B, 5 and 4. There is also a remarkable deposition on the vertical segment of tile 9C just opposite the inner strike point. On other areas of the roof baffle there is only a small deposition, and some erosion at the roof baffle strike point location. The outer strike point and the outer baffle (tiles 2 and 3A) are net carbon erosion area [7, 9]. The carbon erosion cannot be quantified on tiles 1A and 1B due to delamination of the carbon marker. A small deposition area

§ These depths are for amorphous hydrocarbon layers with $D/C = 0.4$ and a density of 1×10^{23} at/cm^3.

Table 1. Amounts of D trapped in different areas of ASDEX Upgrade. If not otherwise indicated, the numbers are for the 2002–2003 discharge campaign. Numbers in brackets are obtained from the amount of deposited B + C, assuming D/(B + C) = 0.4.

Location	Amount of D (g)	
Inner divertor tiles	1.15	(1.84)
Roof baffle tiles	0.16	
Outer divertor tiles	0.14	
Gaps between divertor tiles	0.12	
Below roof baffle	0.46	
Pump ducts	0.005†	
Upper divertor tiles	0.16‡	
Gaps between inner heat shield tiles	0.07	
Auxiliary limiter tiles	0.03§	
Total	**2.30**	**(2.99)**

† during 2001–2002 discharge campaign
‡ during 2003–2004 discharge campaign
§ during 2005–2006 discharge campaign

is observed on the lowest few centimeters of tile 1A.

The deposited layers consist predominantly of C, with 5–40% of B/(B+C). The sum of B+C is obtained from the energy shift of the Re marker peak in the RBS spectra and is accurate within about 10%, while the discrimination between B and C was only possible for thicker layers (which were analyzed with 2.5 MeV protons) and has a larger error bar due to overlap of the RBS spectra from B and C. Boron is deposited during regular boronizations mainly in the main chamber, while boronizations are almost ineffective in the divertor: The deposition of B on divertor tiles during boronizations is small [20]. Boron observed in deposited layers in the divertor therefore originates predominantly from erosion of boron layers in the main chamber and subsequent transport to the divertor.

The deuterium inventory on the divertor tiles after the 2002–2003 campaign is shown in Fig. 3(bottom), magnified views of the inner and outer divertor are shown in Fig. 4 and Fig. 5. The highest inventory is observed at the inner strike point tile 4, where also the largest deposition of B+C occurs. The D/(B+C) ratio is around 0.4 on most areas of this tile. This ratio decreases significantly below 0.4 only in the region s = 510–530 mm (see the lower left panel in Fig. 4). A remarkably high inventory is also observed on the small vertical segment of tile 9C, just opposite the inner strike point. Tile 5 and a fraction of tile 6B show strong deposition of B and C. Tile 6B was analyzed only with 1 MeV ^{3}He, and the ion range is too small to analyze the D-inventory of the whole layer thickness. SIMS measurements indicate a D/(B+C) ratio of 0.2–0.3 on this tile, see Fig. 4. Tile 5 showed a low mean D/(B+C) ratio of 0.1–0.2 in 2002–2003,

as observed both in NRA and SIMS measurements. The dashed line in Fig. 4(bottom left) shows the D inventory, which would be observed for D/(B+C) = 0.4. The SIMS data indicate an increase of the D inventory on tile 5 close to tile 4 (s = 340–360 mm). SIMS depth profiles show an inhomogeneous deuterium depth distribution on tile 5 (see Fig. 6): The depth profile from tile 5 shows a higher D/C ratio within the first micron, and a smaller D/C ratio deeper in the deposit. The depth profile from tile 4 is more homogeneous, and the D/C ratio in larger depths is identical to the surface. The low D/(B + C) ratio on tile 5, as observed in 2002–2003, was not reproduced in 2004–2005: The D inventory was higher, and the D/(B + C) ratio on tile 5 was close to 0.4 after the 2004–2005 campaign, see Fig. 4 (right panel).

The D inventory on roof baffle tiles 9A and 9B is small and in the range 2×10^{17}–2×10^{18} D-atoms/cm^2. The D inventory on outer divertor tiles is also low with 1×10^{17}–1×10^{18} D-atoms/cm^2, and the lowest D inventories are observed at the strike point where also the highest surface temperatures are reached (see Fig. 5). The only mentionable D-inventory in the outer divertor in 2002–2003 was at the lower 5 cm of tile 1A, where the strike point was not positioned. The strike point was occasionally positioned in this area in 2004–2005, resulting in considerably lower inventories in this area after that campaign. Some retention was also observed on tile 10 close to the corner to tile 1A, while the rest of tile 10 was a net carbon erosion area [9] with only small D inventories (Fig. 5, right panel). The campaign-integrated ion fluence to the outer divertor was determined with Langmuir-probes during the 2004–2005 discharge campaign and is shown in Fig. 5 (right panel). The time distribution of strike point positions and the particle fluence distribution are strongly related.

The surface temperature history of the inner and outer strike point tiles in 2002–2003 is shown in Fig. 7. The maximum surface temperature reaches 1800 K, but only for short time intervals of a few ms during ELM's. The maximum surface temperature averaged over 50 ms usually stays below 1000 K at the inner strike point, while the outer strike point gets hotter and reaches a maximum of 1500 K for more than 50 ms. The mean tile surface temperature during a whole discharge usually stays below 600 K, with a tendency of the outer strike point tiles to higher mean temperatures than the inner strike point tiles.

The total detected amount of D on tiles 6A, 6B and 5 was 0.24 g after the 2002–2003 campaign, compared to 0.62 g after the 2004–2005 campaign. The higher amount in 2004–2005 is partly due to the higher analyzing energy on tile 6B, which detects D in the whole deposited layer thickness, and partly due to the higher D/(B+C) ratio on tile 5. The amount of deposited B+C on tiles 6A, 6B and 5 was 13.4 g in 2002–2003, compared to 9.9 g in 2004–2005: This reflects the smaller discharge time in 2004–2005.

The total amounts of deposited D on divertor tiles are obtained by assuming toroidal symmetry. They are summarized in Table 1. Numbers in brackets are obtained from the amount of deposited B + C on tiles 6B and 5, assuming a D/(B + C) ratio of 0.4. This number is an upper boundary for the possible amount of codeposited D on the tiles and was reached in 2004–2005, but not in 2002–2003. A considerably larger ratio than about

0.4 is also hard to imagine under the ASDEX Upgrade divertor plasma conditions.

3.2. Gaps between divertor tiles

ASDEX Upgrade divertor tiles are separated by gaps with a width of 6–8 mm. The D-inventory at the side faces of inner divertor tiles 5 and 6B, and outer divertor tile 2 was measured after the 2004–2005 campaign, the distribution for tile 5 is shown in Fig. 8. Retention in the gaps is highest at the plasma exposed side at the gap entrance, where the deuterium areal density is about 2–3 times higher than at the tile surface. The deposited amount decreases exponentially with a decay length of a few millimeters when moving deeper into the gap. The inventory at the shadowed side is considerably lower than at the plasma-exposed side and decays with a decay length of about 20–30 mm, the inventory deep in the gap is small on both sides. Qualitatively similar results for gaps between tungsten tiles were already obtained in [21].

In the gaps of outer divertor tile 2, see Fig. 9, a maximum surface density of 5×10^{17} D-atoms/cm^2 was observed (compared to about 4×10^{17} D-atoms/cm^2 at the tile surface). The inventory was almost identical at the plasma-exposed and the plasma-shadowed tile sides, and decreased with a decay length of about 20–30 mm. The inventory deeper in the gap was only about 1×10^{17} D-atoms/cm^2. The strike point tiles 1A and 1B have almost no gaps, so that the inventory in gaps of outer strike point tiles is assumed to be also small. The total inventory trapped in gaps in the outer divertor is therefore negligible compared to the inventory in the inner divertor.

These results differ from [21], where a W gap sample was exposed with the divertor manipulator between tiles 1A and 1B. A maximum amount of 2.5×10^{17} D-atoms/cm^2 was observed after only 3 discharges, having a total discharge time of 17 s. This would extrapolate to more than 4×10^{19} D-atoms/cm^2 for the whole discharge campaign, which is by two orders of magnitude higher than the amount which we observe on tile 2 (but comparable to the gap retention at tile 5). This difference may be due to the different materials in the surrounding: The gap sample was exposed at the outer strike point tile 1, which consisted of carbon, while tiles 2 and 3 were coated with tungsten. The carbon ambience of the gap sample may have resulted in an increased carbon deposition.

The D inventory in the gap of a single tile 5 is about 770 μg. This has to be compared to the amount of D, which would have been deposited without gap, i.e. if the tile would be continuous. This amount can be derived from the amount of D deposited at the tile surface and the gap width and is about 940 μg, i.e. *larger* than with the existing gap. For tile 6B the amount of D deposited in the gap is about 130 μg, compared to about 200 μg without gap. This indicates that gaps between inner divertor tiles do not increase the D inventory in ASDEX Upgrade, but only result in a different spatial distribution.

The D-inventory trapped in gaps during the 2002–2003 campaign was derived by using the measured values for tiles 6B and 5 from the 2004–2005 campaign, and by extrapolating the amount of D at the tile surface with a decay length of 2 mm for tiles

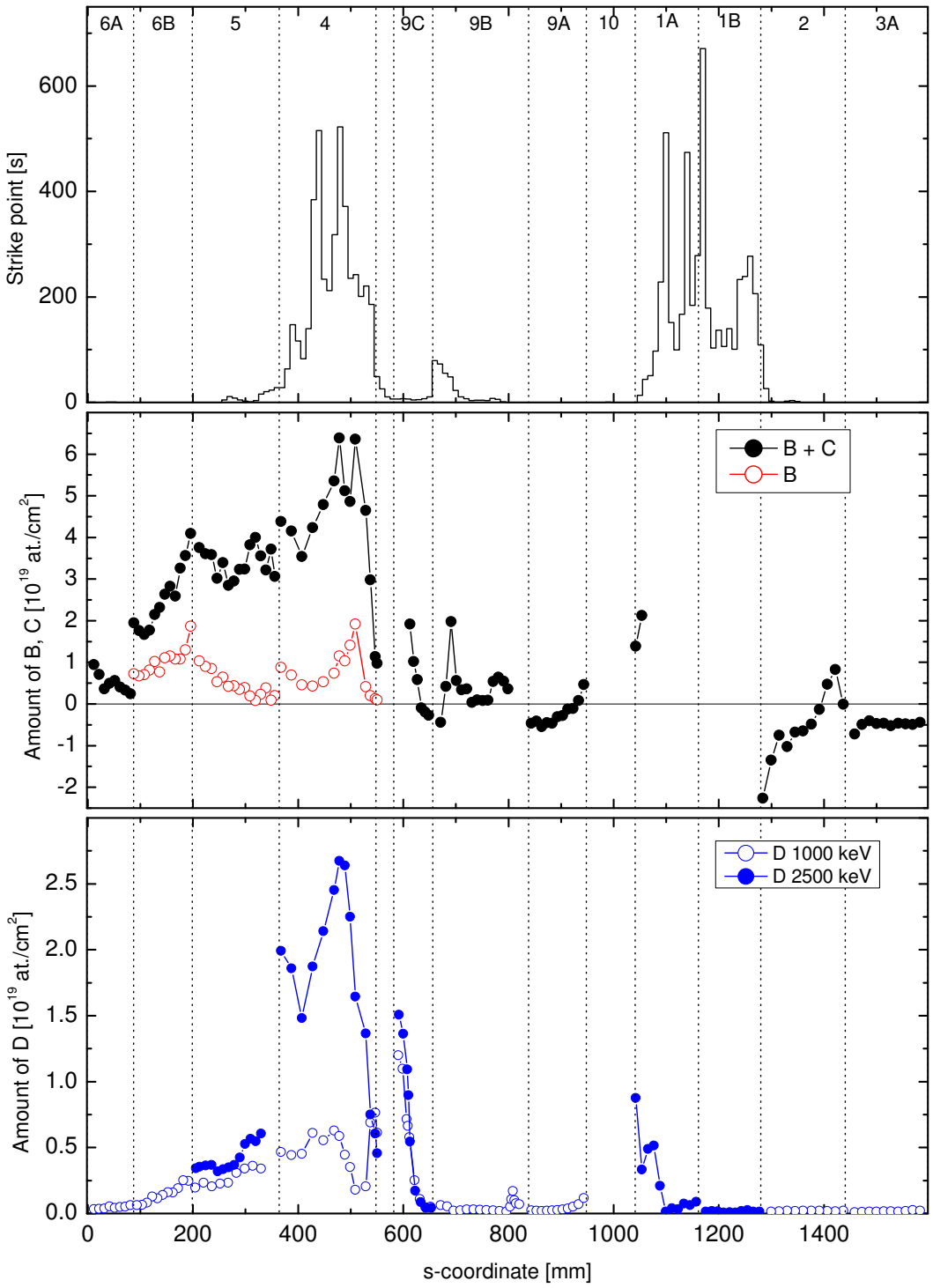

Figure 3. Strike point position and deposition of B, C and D during the 2002–2003 campaign. Top panel: Distribution of strike-point positions. Middle panel : Net deposition and erosion of boron and carbon. Positive numbers are deposition, negative numbers are erosion. Bottom panel: Co-deposition of deuterium, measured with 1.0 and 2.5 MeV ^{3}He ions, corresponding to information depths of 2 and 10 μm. An extended view of the inner divertor deposition is shown in Fig. 4, the outer divertor is shown in Fig. 5.

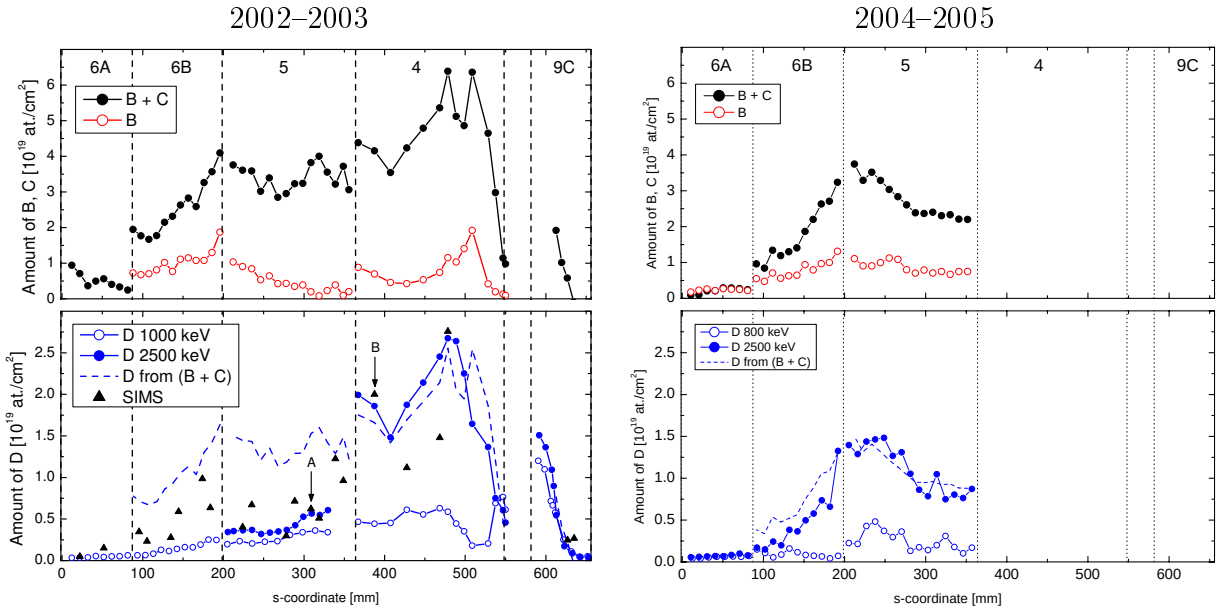

Figure 4. Deposition of B, C and D during the 2002–2003 and 2004–2005 discharge campaigns in the inner divertor. Left panels: 2002–2003 campaign; right panels: 2004–2005 discharge campaign. Top panels: Deposition of boron and carbon. Bottom: Co-deposition of deuterium. Dots: Measured values at 1.0 or 0.8 and 2.5 MeV. Dashed lines: Deuterium inventory derived from the amount of (B + C) assuming D/(B + C) = 0.4. Triangles: Amount of D derived from the D/^{12}C SIMS signal. This amount is in arbitrary units and adjusted for best fit to the NRA results. SIMS depth profiles from positions A and B are shown in Fig. 6.

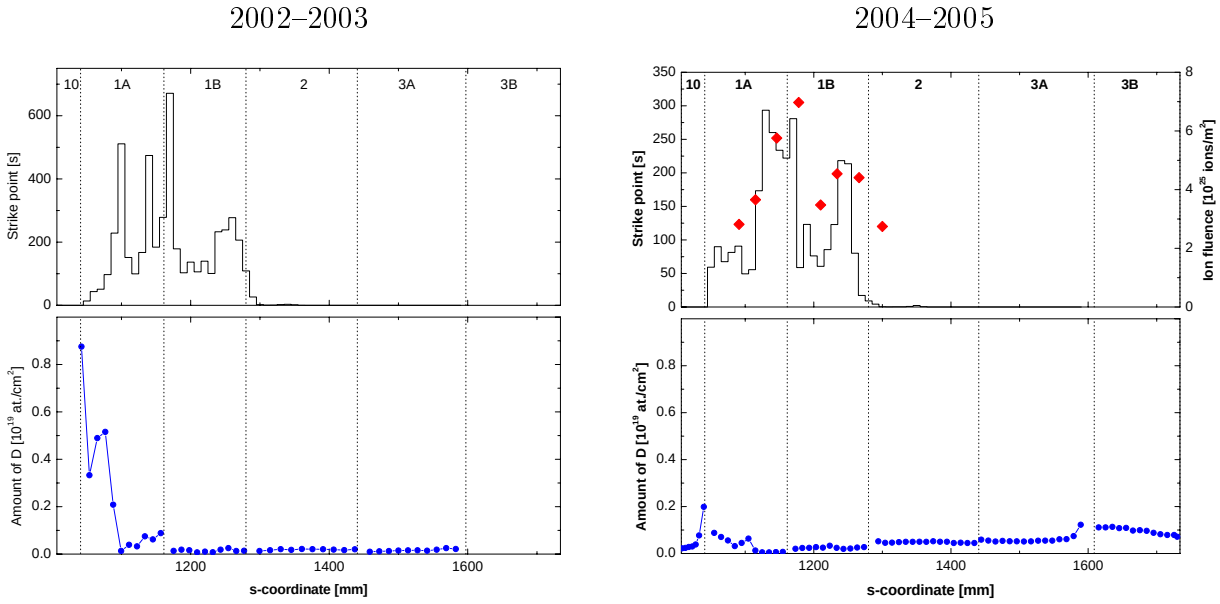

Figure 5. Deuterium inventory during the 2002–2003 and 2004–2005 discharge campaigns in the outer divertor. Left panels: 2002–2003 campaign; right panels: 2004–2005 discharge campaign. Top panels: Strike point position. The right hand panel also shows the ion fluences to the outer divertor in 2004–2005 (diamonds). Bottom: Deuterium inventory.

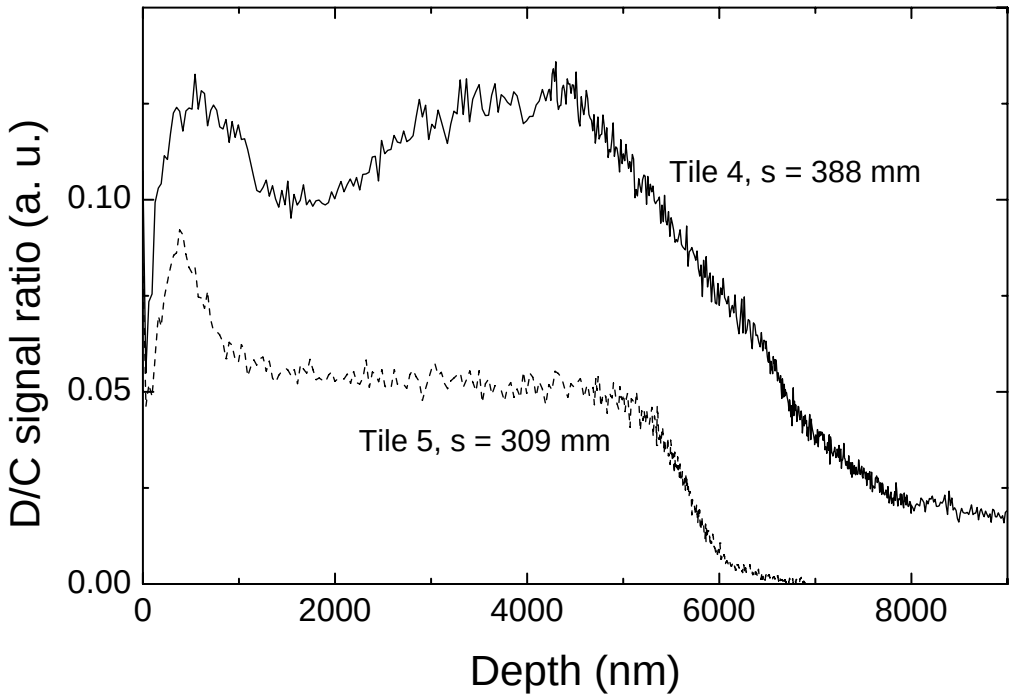

Figure 6. SIMS depth profiles of the D/C ratio from positions A (s = 309 mm) and B (s = 388 mm), see Fig. 3.

4 and 6A. This is justified because the amounts of deposited B+C on tiles 6A, 6B and 5 are not too different for the 2002–2003 and 2004–2005 campaigns, see Fig. 4. A decay length of about 2 mm was observed on tiles 5 and 6B, see above. The gap inventory is about 0.12 g (table 1), which is less than 10% of the amount trapped on the tile surfaces.

3.3. Below the roof baffle

The co-deposition of hydrocarbon layers below the roof baffle and in other remote areas without direct plasma contact was studied with silicon long term samples [11, 22, 23, 24]. The co-deposition of D on the samples is shown in Fig. 10, the carbon deposition can be found in [22]. Amorphous deuterated hydrocarbon layers with D/C = 0.4–1.0 are found on the samples [11, 23, 24]. In total about 0.46 g D were codeposited below the roof baffle during the 2002–2003 campaign. As can be seen in Fig. 10, the largest inventories are observed on samples with direct line-of-sight to the divertor strike points. Samples facing the inner divertor show larger inventories than samples in the outer divertor. As was already shown in [24] with cavity samples, layers in remote areas are mainly formed by particles with high surface loss probabilities, i.e. layers are mainly formed at the surface where the first wall collision takes place. Because these particles (which may be hydrocarbon radicals, carbon atoms, or small carbon clusters) originate mainly from the divertor strike points, codeposited layers are formed predominantly on surfaces with line-of-sight to the strike points. As a result larger inventories are formed on tile 9C

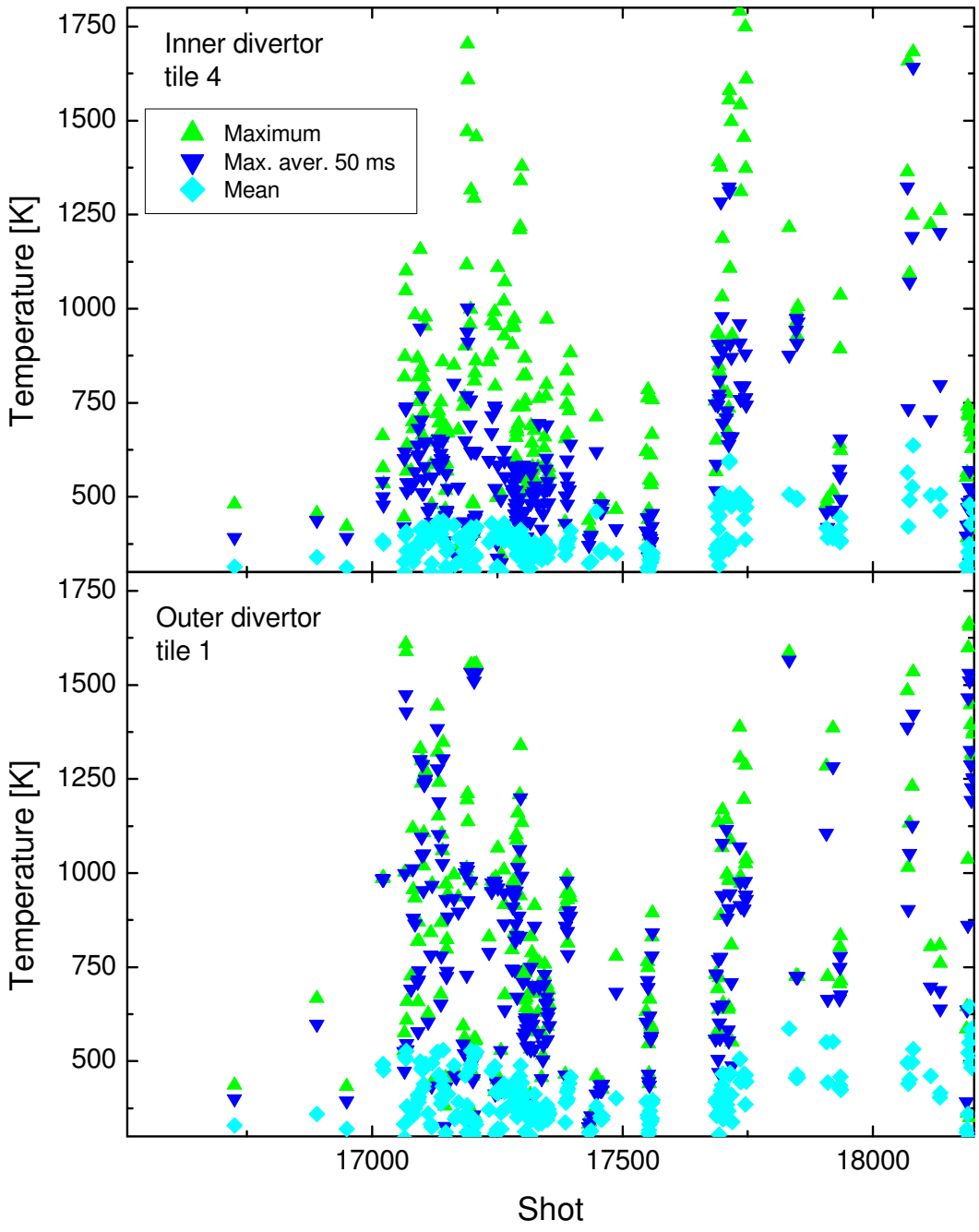

Figure 7. Surface temperature history of the inner and outer strike point tiles during the 2002–2003 discharge campaign. Up triangles: Maximum surface temperature during a discharge; Down triangles: Maximum average surface temperature (averaged over 50 ms) during a discharge; Diamonds: Mean surface temperature averages over the whole tile and the whole discharge.

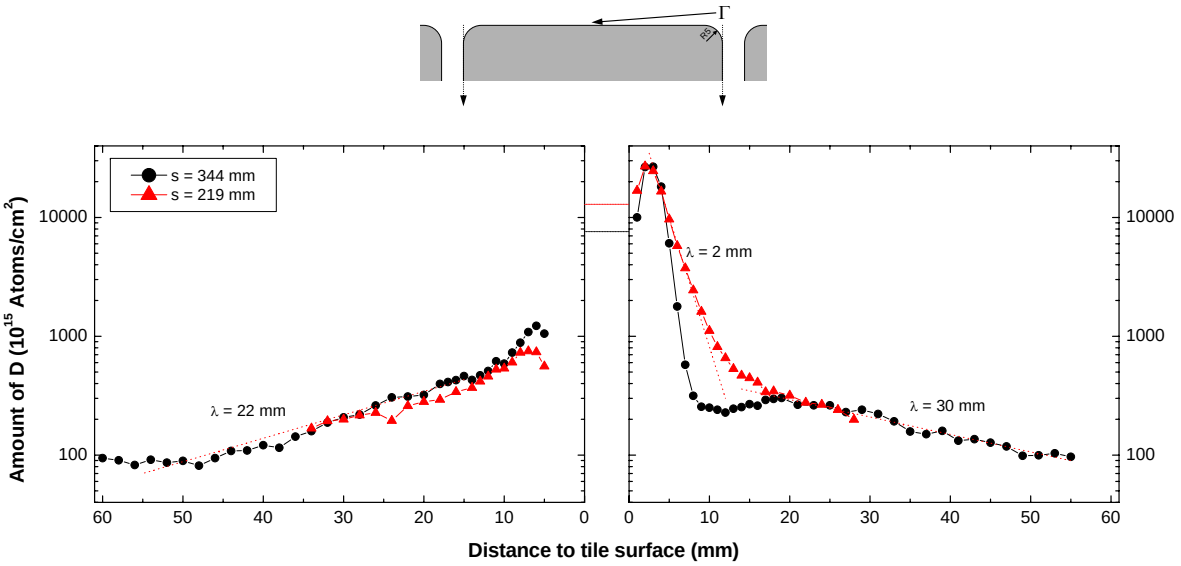

Figure 8. Deuterium inventory in gaps between inner divertor tile 5 at two different poloidal positions after the 2004–2005 campaign. Top: Geometry of the gaps. Dotted arrows indicate the lines of analysis, the direction of the incident flux Γ is also indicated. Bottom: Deuterium inventory on the left and right side faces of tile 5. Dashed lines between the figures are the inventory on the plasma-exposed tile surface. Dotted lines indicate an exponential decay with decay length λ. These lines are only to guide the eye.

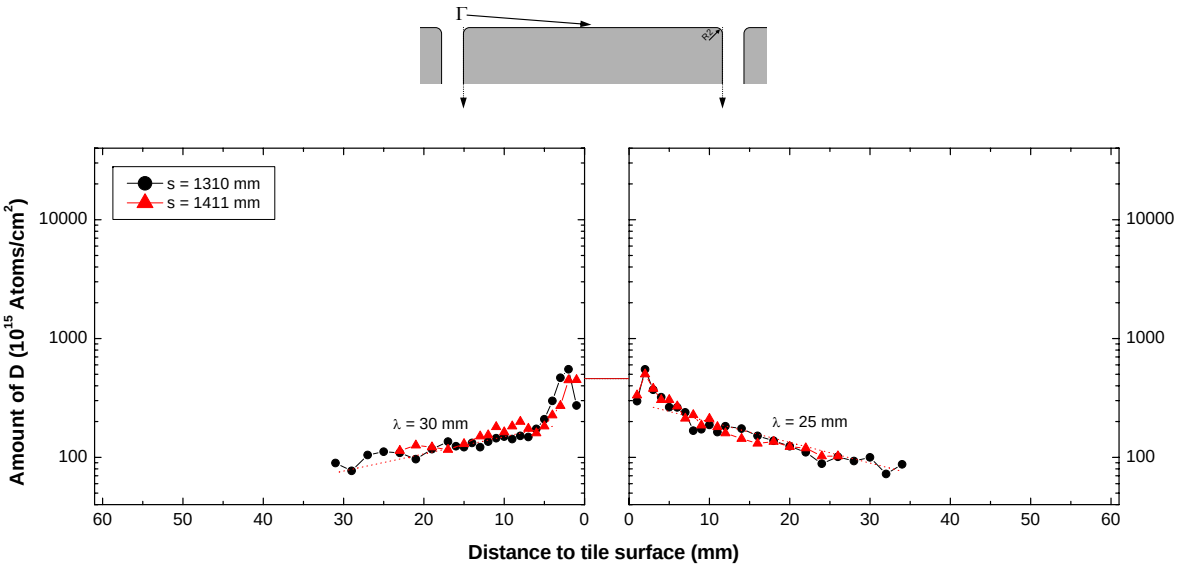

Figure 9. Deuterium inventory in gaps between outer divertor tile 2 at two different poloidal positions after the 2004–2005 campaign. Top: Geometry of the gaps. Dotted arrows indicate the lines of analysis, the direction of the incident flux Γ is also indicated. Bottom: Deuterium inventory on the left and right side faces of tile 2. Dashed lines between the figures are the inventory on the plasma-exposed tile surface. The scale is identical to Fig. 8. Dotted lines indicate an exponential decay with decay length λ. These lines are only to guide the eye.

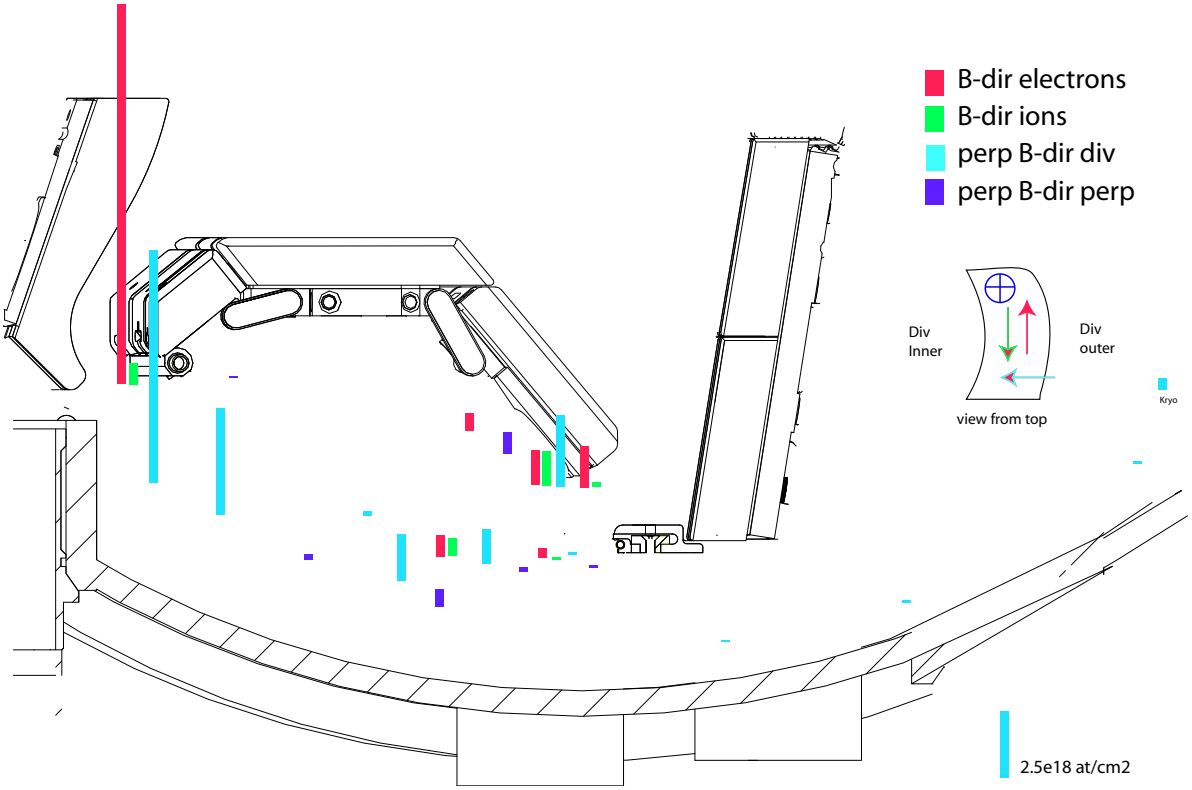

Figure 10. Deuterium inventory below the roof baffle and at the pump duct entrance. The height of the bar shows the amount of D (see lower right corner for scale), the color of the bar indicates the orientation of the sample. The carrier structure below the roof baffle has been neglected.

and on all surfaces (carrier structure etc.) below the roof baffle with direct line-of-sight to the inner and outer strike points. In addition to these particles with high surface loss probability a flux of particles with lower surface loss probability is observed [24]. Particles with low surface loss probability can survive several wall collisions and are responsible for hydrocarbon layer growth in areas without direct line-of-sight to the plasma or to the strike points. Therefore some hydrocarbon layer growth is also observed in shadowed areas, see Fig. 10, but the layer thicknesses and the total D inventory in these shadowed areas are much smaller than in areas with direct line-of-sight to the strike points.

3.4. Pump ducts

The layer co-deposition in the pump ducts of ASDEX Upgrade was investigated during the 2000–2001 discharge campaign with long term samples [11]. The total co-deposition of D in all 14 pump ducts was only about 0.002 g. This low co-deposition was confirmed with another set of samples during the 2001–2002 discharge period, where a total amount of deuterium of about 0.005 g was deposited during the campaign. A piece from a flange located in a pump duct and exposed from 1996-2006 for about 10 years

showed a D inventory of only 2×10^{15} atoms/cm^2, which is in line with the small co-deposition observed on the long term samples. From these repeated measurements it can be concluded that deuterium co-deposition in the pump ducts of ASDEX Upgrade is negligible.

3.5. Upper divertor

The retention of D in the upper divertor and on the upper passive stabilizer loop (PSL) protection tiles was studied by analyzing a poloidal section of upper limiter and PSL protection tiles. The tiles were exposed in the 2003–2004 campaign, during which 232 s of plasma in upper divertor configuration were performed. The deuterium inventory of these tiles is shown in Fig. 11 together with the strike point distribution. The maximum inventory is about 2×10^{18} D-atoms/cm^2, while the inventory on most of the tiles reaches only 2–4$\times 10^{17}$ D-atoms/cm^2. Boronizations are effective in the upper divertor and deposit about 50–100 nm a-B:C:D layers on the tiles during each boronization [20, 25], so that some fraction of the detected D originates from boronizations and not from layer deposition during plasma operation. The upper strike point areas show the lowest inventories, while some material deposition and higher deuterium inventories are observed a few centimeter inwards of the inner and outwards of the outer strike point. The total D inventory in the upper divertor is about 0.16 g, see table 1, which is less than 7% of the total inventory of ASDEX Upgrade.

3.6. Gaps between inner heat shield tiles

The inner heat shield is a net erosion area, but large influxes of carbon were observed there even after coating with tungsten [26]. This shows that the inner heat shield is an important carbon recycling area. The retention in the gaps between inner heat shield tiles was measured during the 2002–2003 campaign with five long term samples (LTS). The LTS were placed in the tile gaps, where a total of about 0.07 g deuterium is found in codeposited layers (table 1).

3.7. Main chamber limiters

3.7.1. Auxiliary limiters ASDEX Upgrade has four auxiliary limiters at the low field side in the main chamber. Each limiter consists of 9 tiles, see the poloidal section in Fig. 12. The deuterium inventories were determined after the 2005–2006 campaign on 3 tiles from the limiter in sector 16/1 (tile 1 from the top, tile 4 close to the midplane, and tile 8 from the bottom of the limiter) and on one tile of the limiter in sector 14/15 (tile 2). The deuterium distributions are shown in Fig. 12 for the tiles from sector 16/1. These limiters are net erosion areas [27], so only minor D inventories are expected. The measured D inventory is in the range 4×10^{17} to 2×10^{18} D-atoms/cm^2. In total about 0.03 g D were detected on all 4 limiters (Table 1). The D was always associated with boron, which may indicate that the detected D and B are at least partly remnants of

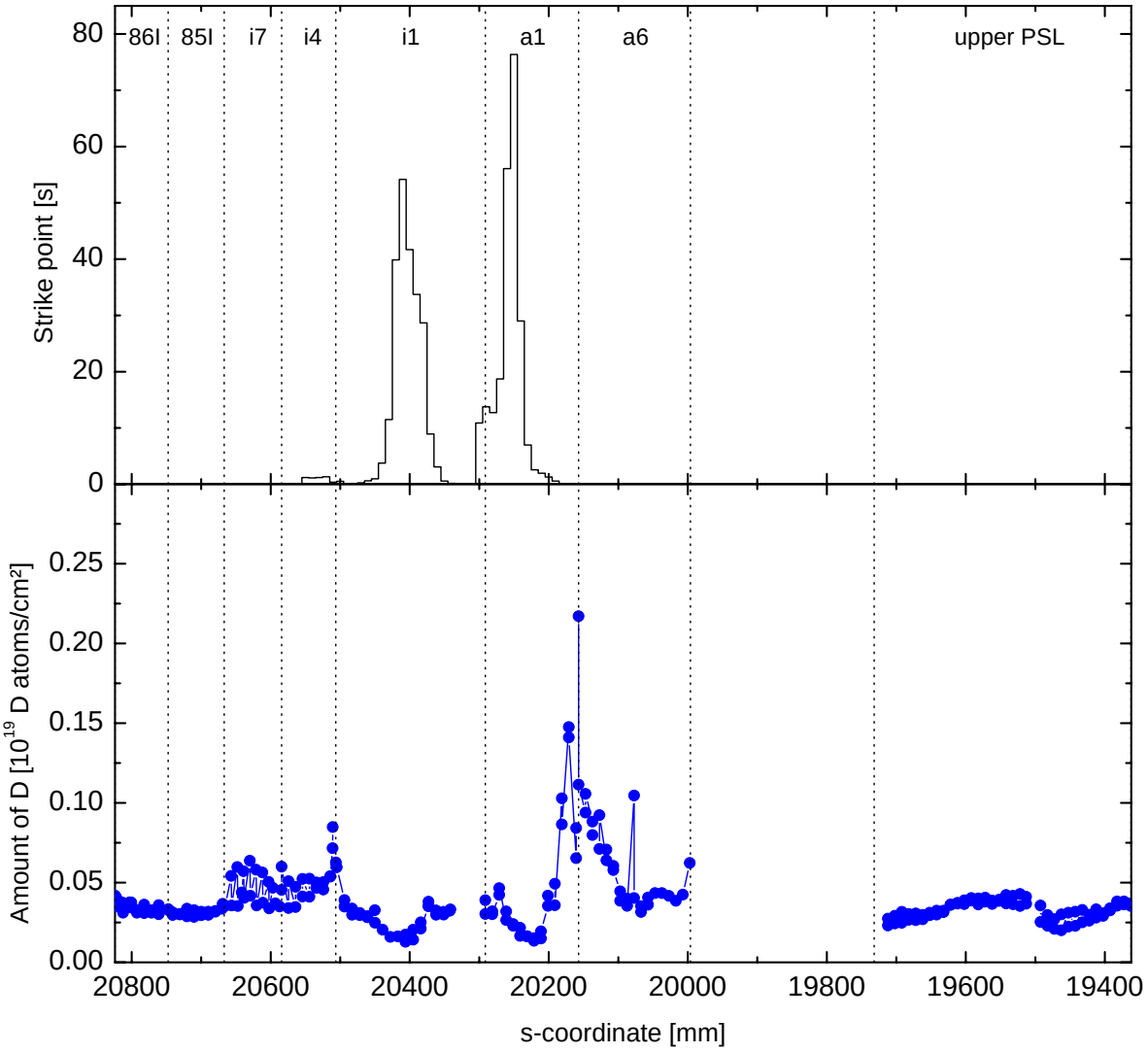

Figure 11. Strike point position and deuterium inventory at upper divertor and upper PSL protection tiles after the 2003–2004 campaign. Top panel: Distribution of strike-point positions; bottom panel: D inventory. Numbers are tile numbers, see Fig. 1 for the geometry.

layers deposited during boronizations. The limiters are tilted by 11° in toroidal direction, see Fig. 12. Tile 4 shows a dip in the inventory at the cusp of the limiter, where the limiter is closest to the plasma and receives the highest particle and power fluxes.

The 2005–2006 campaign is not fully comparable to earlier campaigns due to an almost full tungsten coverage of the main chamber in 2005–2006. This increased tungsten coverage resulted in a decrease of the divertor carbon deposition and deuterium retention by a factor of more than five [28], and it is possible that the increased tungsten coverage also resulted in a decreased deposition at the main chamber limiters by the same factor. The limiter inventory given in Table 1 therefore may be not representative for earlier campaigns. Nevertheless, this uncertainty does not strongly influence the

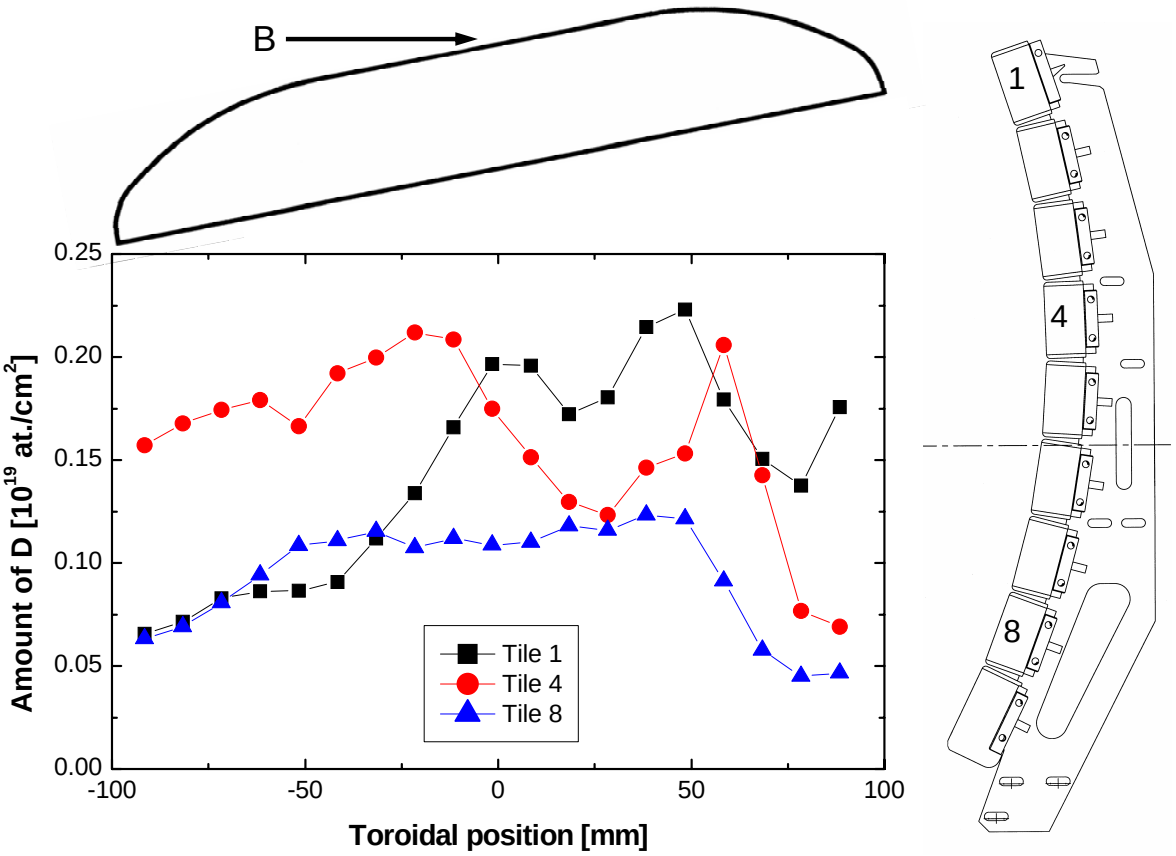

Figure 12. Deuterium inventory at three tiles from the auxiliary limiter in sector 16/1 after the 2005–2006 campaign. A poloidal section of the limiter is shown on the right hand side. The analyzed tiles are indicated by tile numbers, the machine mid-plane is indicated by a dot-dashed line. A toroidal cross-section of the tiles is shown in the upper panel. The tiles are tilted in toroidal direction, and the arrow indicates the direction of the magnetic field B.

total deuterium balance due to the small inventory of the limiters.

3.7.2. ICRH limiters The main chamber contains four rectangular ICRH antennae, which are protected by limiters at all four sides. These limiters are net erosion areas [27]. The deuterium inventory of these limiters was not determined. Optical inspection of the tiles showed no indication for thick deposits, and the surface temperature of these limiters goes beyond 900 K during many discharges, so it is assumed that the D inventory of these limiters is small.

3.8. Deuterium input

The deuterium input into the ASDEX Upgrade vessel during the 2002–2003 discharge campaign is summarized in Table 2. The table contains only deuterium which was introduced during plasma discharges, while deuterium gas puffs during non-plasma operation (e.g. gas puffs for calibration purposes of diagnostics and the like) were

Table 2. Deuterium input during the 2002–2003 campaign.

	Amount of D (g)
Gas inlet	66.4
Neutral beams	7.3
Pellets	1.7
Boronizations	3.7
Total	**79.1**

excluded: this gas is pumped and does not stay in the vessel.

Deuterium is fuelled into plasma discharges by gas puffs, neutral beams and pellets. An additional deuterium input are boronizations, which are performed in a mixture of 10% deuterated diborane B_2D_6 and 90% He and create deuterated amorphous boron or boron/carbon layers at the vessel walls [20, 25]. The layers contain D at a ratio of D/B = 0.3–0.5, the layer thickness deposited during each boronization is about 50–100 nm. These layers can be subsequently eroded during plasma discharges, and the D is able to fuel discharges. During each boronization about 4.2×10^{23} B-atoms are deposited at the walls [25], resulting in a total D-input of about 3.7 g in 6 boronizations (table 2).

The total deuterium input during the 2002–2003 campaign was about 79.1 g, see table 2. For comparison: The 2004–2005 campaign was shorter, and the total deuterium input during that campaign was about 46.1 g.

4. Discussion

As can be seen from Tables 1 and 2, the measured amount of retained D was about 2.3 g during the 2002–2003 campaign, compared to a total D input of 79.1 g. This corresponds to a retention of 3.0% of the D input. As already discussed in section 3.1, the measured amounts of D on tiles 5 and 6B during the 2002–2003 were smaller than during the 2004–2005 campaign. The amount of D, which can be potentially retained in codeposited layers, can be obtained from the amount of B + C and the assumption of D/(B + C) = 0.4, resulting in a total D inventory of about 3.0 g. This corresponds to a retention of 3.9% of the D input. This marks the upper limit, and the actually observed retention may be somewhat lower, as observed during the 2002–2003 campaign.

The majority of the deuterium inventory (about 70%) is found on inner divertor tile surfaces, especially at the inner strike point tile 4 (see table 1). About 20% are found in areas without direct plasma contact, such as on the roof baffle tile 9C and below the roof baffle. Most of this co-deposition is in direct line-of-sight to the strike points, especially in line-of-sight to the inner strike point. Co-deposition in gaps between tiles is also predominantly at or close to plasma exposed areas. Some retention is observed in shadowed areas without direct line-of-sight to the plasma or deeper in gaps, but the

inventory in these areas is small. The inventory in very remote areas like pump ducts is negligible.

This distribution pattern can be explained in the following way: Codeposited hydrocarbon layers are predominantly formed in the inner divertor at locations with direct plasma impact, i.e. at areas with high incident fluxes of carbon and deuterium. Some fraction of these redeposited layers are subsequently re-eroded, as was already shown at JET [29]. The erosion products then form layers mainly at areas with direct line-of-sight to the area of origin, i.e. their surface loss probability is high. A small fraction of the erosion products (most probably hydrocarbon radicals) has a smaller surface loss probability, and is therefore able to survive several wall collisions. These particles form layers in shadowed areas. Particles with very low surface loss probabilities of the order of 10^{-3} are able to migrate into the pump ducts, but their contribution to the D inventory is negligible. This is most probably due to re-erosion by atomic hydrogen [24]. Surface loss probabilities have been measured in [24] and confirm this interpretation.

Most of the outer divertor is a net erosion area for carbon and tungsten [7, 9], and surface temperatures can get higher than in the inner divertor. Consequently the deuterium retention in the outer divertor is small. The detailed distribution of D depends on the distribution of strike point positions during the discharge campaign. A small co-deposition area is usually observed in the corner between tile 10 and tile 1A.

The error bar due to inaccuracies of the analysis and due to the extrapolation from a specific toroidal location to the whole machine is estimated to be below 50%, so that the D retention from our post-mortem surface analysis is in the range 2–6% of the deuterium input. This retention still may somewhat underestimate the total retention due to formation of hydrocarbon layers in areas which were not analyzed. Because all major areas with plasma contact and also many areas without direct plasma contact were included in the analysis, this additional inventory in non-analyzed areas probably does not increase the inventory substantially. A release of about 17% of trapped tritium was observed during exposure to air after the DTE1 campaign at JET [30]. Some loss of deuterium during air exposure may have also occurred at ASDEX Upgrade. The value observed at JET is probably an upper bound for the outgassing at ASDEX Upgrade: The layers at JET are more deuterium-rich (with D/C of about 0.8) and probably less stable than the ASDEX Upgrade layers.

This inventory from surface analysis has to be compared to gas balance measurements performed during the same experimental campaign at ASDEX Upgrade, which yield a retention of 10–20% [31]. Because the gas balance is the difference of two alike numbers, the error of these numbers is within a factor of about two. Post-mortem surface analysis generally has a tendency to underestimate the D retention: Not all D-containing areas can be analyzed, and outgassing during singular high power discharges and venting to air may occur. Gas balance has a tendency to overestimate the inventory due to limited integration time for wall outgassing between discharges and during week-ends. Keeping these error bars in mind, both methods agree marginally at a retention

level of 5–6%.

Gas balance will be an important diagnostic during the initial hydrogen and deuterium operation phases of ITER, and results obtained during these phases will have to be extrapolated to the tritium phase. It should be kept in mind, that according to the ASDEX Upgrade experience a gas balance may overestimate the hydrogen retention.

A significant difference between gas balance and post-mortem surface analysis has been observed at Tore Supra. It has been proposed that this difference may be explained by deep diffusion of D into carbon fibre composite (CFC) material [32, 33]. This deep diffusion has been shown experimentally in laboratory experiments [34]. However, while at Tore Supra the whole CIEL limiter is made from CFC and exposes large CFC surfaces to the plasma, the use of CFC is limited to the inner strike point tile 4 in ASDEX Upgrade. As shown in section 3.1, this is a net deposition area which is coated with many μm of deposited hydrocarbon layers. Surface temperatures reach high values only for very short time intervals. Diffusion of D in CFC should not play a large role in ASDEX Upgrade due to the limited CFC area and the limited time interval at high surface temperatures.

The lateral distributions of retained D are qualitatively similar in JET and in ASDEX Upgrade. The outer divertors are net erosion areas in both machines [35, 9]. D is predominantly trapped in the inner divertor, both on divertor tiles and in remote areas in line-of-sight to the inner strike point [29]. These remote areas are the inner divertor louvers at JET, and the roof baffle at ASDEX Upgrade.

Simulation calculations of carbon erosion and re-deposition predict a mixture of net erosion and net deposition areas for the inner and outer ITER divertors [36], and "inner and outer divertor contribute similar amounts to the overall tritium retention in carbon layers" [36]. Such a distribution is not observed at ASDEX Upgrade or JET. However, ITER will require more balanced plasma parameters in the inner and outer divertors than today's experiments due to power and particle loads, so that the distribution of net erosion and deposition areas may be different than observed today. The overall deuterium retention and the lateral distribution of codeposited layers in existing experiments should be taken as a benchmark for computer codes, which are used for predictions of the tritium retention in ITER.

5. Conclusions

The deuterium inventory in different areas of ASDEX Upgrade was determined between the years 2002 and 2005. The analysis included plasma exposed and remote areas in the lower and upper divertors and in the main chamber. About 70% of the retained D is found on inner divertor tiles, and about 20% in areas at or below the roof baffle with direct line-of-sight to the strike points. Trapping of D in very remote areas like pump ducts is negligible. The amount of D found in gaps between inner divertor tiles does not exceed the amount expected for continuous tiles without gaps: Gaps in ASDEX Upgrade therefore do not increase the deuterium retention, but only result in a different lateral

distribution. The deuterium inventory in the outer divertor depends on the distribution of strike point positions, but is generally much smaller than in the inner divertor.

The measured deuterium retention for the 2002–2003 campaign is about 3.0% of the D input. An upper boundary for the possible D inventory can be obtained from the amount of deposited B + C and assuming a D/(B + C) ratio of 0.4. This marks the maximum possible retention, which is about 4% of the D input. This value can be obtained if the surface temperature of divertor tiles with heavy deposition does not exceed about 600 K for longer time intervals. The surface temperatures of inner and outer divertor tiles show short surface temperature excursions up to 1800 K with a duration of a few ms during ELM's. These surface temperature excursions do not decrease the observed D inventory on the tile surfaces significantly.

These results from post-mortem surface analysis are lower than the results obtained from gas balance measurements, which give a D retention of 10–20% [31]. Taking the error bars of the investigations into account, both methods agree at a retention level of 5–6%. Gas balance will be an important diagnostic during the hydrogen and deuterium phases of ITER. It has to be kept in mind that this method may overestimate the retention.

Simulation calculations of tritium retention in ITER predict an almost equal contribution of the inner and outer divertor to the hydrogen inventory [36]. This distribution is much different than observed in today's machines. The overall deuterium retention and the lateral distribution of codeposited layers in existing experiments should be used as a benchmark for computer codes, which are used for predictions of the tritium retention in ITER. The majority of trapped D is observed at the surfaces of inner divertor tiles in ASDEX Upgrade. About 20% of the deuterium is trapped in remote areas in ASDEX Upgrade, but predictions for ITER are difficult due to the higher surface temperatures. Retention in gaps also plays only a minor role in ASDEX Upgrade. This may be different in ITER due to higher surface temperatures of tiles and lower temperatures in gaps due to the proximity to water cooling structures. ITER will require a tritium fuelling of about 50 g for a 400 s discharge [37]. A retention of 3–4%, similar to what is observed in ASDEX Upgrade, would result in a tritium retention of about 1.5–2 g T per discharge. This is at the lower end of the predicted band of values, which range from 2–6 g T per discharge for the foreseen Be/C mixture [36] and 13 g T per discharge for a full carbon ITER [36]. But even the projected ASDEX Upgrade result is still about one order of magnitude higher than the acceptable long term tritium retention for ITER [38]. However, the ASDEX Upgrade data were gathered in a carbon dominated machine with cold walls. ITER will contain less carbon, and the divertor tiles, where most of the hydrogen retention is observed, will have higher surface temperatures, resulting in a decrease of the retention. The ASDEX Upgrade data therefore may mark an upper limit for the expected tritium retention in ITER.

Acknowledgments

Ion beam analysis measurements by T. Utikal, F. Blobner, B. Tyburska and H. Kulinski, the technical assistance by J. Dorner and M. Fußeder, and helpful discussions with H. Maier (Garching) and A. Kirschner (Jülich) are gratefully acknowledged.

References

[1] VIETZKE, E. and HAASZ, A., Chemical erosion, in *Physics of Plasma-Wall Interactions in Controlled Fusion*, edited by HOFER, W. and ROTH, J., page 135, Academic Press, San Diego, New York, Boston, London, Sydney, Tokyo, Toronto, 1996.

[2] BALDEN, M. and ROTH, J., J. Nucl. Mater. **280** (2000) 39.

[3] MAYER, M., PHILIPPS, V., WIENHOLD, P., ESSER, H., VON SEGGERN, J., et al., J. Nucl. Mater. **290-293** (2001) 381.

[4] FEDERICI, G., ANDERL, R., ANDREW, P., BROOKS, J., CAUSEY, R., et al., J. Nucl. Mater. **266-269** (1998) 14.

[5] FEDERICI, G., BROOKS, J., COSTER, D., JANESCHITZ, G., KUKUSKHIN, A., et al., J. Nucl. Mater. **290-293** (2001) 260.

[6] NEU, R., BOBKOV, V., DUX, R., KALLENBACH, A., PüTTERICH, T., et al., J. Nucl. Mater. **363-365** (2007) 52.

[7] MAYER, M., ROHDE, V., LIKONEN, J., VAINONEN-AHLGREN, E., KRIEGER, K., et al., J. Nucl. Mater. **337-339** (2005) 119.

[8] LEHTO, S., LIKONEN, J., COAD, J., AHLGREN, T., HOLE, D., et al., Fusion Eng. Des. **66-68** (2003) 241.

[9] MAYER, M., ROHDE, V., RAMOS, G., VAINONEN-AHLGREN, E., LIKONEN, J., et al., Physica Scripta **T128** (2007) 106.

[10] ROHDE, V., MAIER, H., KRIEGER, K., NEU, R., PERCHERMAIER, J., et al., J. Nucl. Mater. **290-293** (2001) 317.

[11] MAYER, M., ROHDE, V., VON KEUDELL, A., and the ASDEX Upgrade Team, J. Nucl. Mater. **313-316** (2003) 429.

[12] MAYER, M., SIMNRA user's guide, Technical Report IPP 9/113, Max-Planck-Institut für Plasmaphysik, Garching, 1997.

[13] MAYER, M., SIMNRA, a simulation program for the analysis of NRA, RBS and ERDA, in *Proceedings of the 15th International Conference on the Application of Accelerators in Research and Industry*, edited by DUGGAN, J. L. and MORGAN, I., volume 475 of *AIP Conference Proceedings*, page 541, Woodbury, New York, 1999, American Institute of Physics.

[14] MAYER, M., Nucl. Instr. Meth. B **194** (2002) 177.

[15] CHIARI, M., GIUNTINI, L., MANDò, P., and TACCETTI, N., Nucl. Instr. Meth. B **184** (2001) 259.

[16] GURBICH, A., Nucl. Instr. Meth. B **129** (1997) 311.

[17] GURBICH, A., Nucl. Instr. Meth. B **136-138** (1998) 60.

[18] ALIMOV, V. K., MAYER, M., and ROTH, J., Nucl. Instr. Meth. B **234** (2005) 169.

[19] VAINONEN-AHLGREN, E., LIKONEN, J., RENVALL, T., ROHDE, V., NEU, R., et al., J. Nucl. Mater. **337-339** (2005) 55.

[20] ROHDE, V., NEU, R., DUX, R., HÄRTL, T., MAIER, H., et al., Comparison of boronization and siliconization in ASDEX Upgrade, in *26th EPS Conference on Controlled Fusion and Plasma Physics*, volume 23J of *europhysics conference abstracts*, page 1513, 1999.

[21] KRIEGER, K., JACOB, W., RUDAKOV, D., BASTASZ, R., FEDERICI, G., et al., J. Nucl. Mater. **363-365** (2007) 870.

[22] ROHDE, V., MAYER, M., LIKONEN, J., NEU, R., PÜTTERICH, T., et al., J. Nucl. Mater. **337-339** (2005) 847.
[23] ROHDE, V., MAYER, M., and ASDEX Upgrade Team, Physica Scripta **T103** (2003) 25.
[24] MAYER, M., ROHDE, V., and ASDEX Upgrade Team, Nucl. Fusion **46** (2006) 914.
[25] ROHDE, V., DUX, R., KALLENBACH, A., KRIEGER, K., NEU, R., et al., J. Nucl. Mater. **363-365** (2007) 1369.
[26] PüTTERICH, T., DUX, R., GAFERT, J., KALLENBACH, A., NEU, R., et al., Plasma Phys. Controlled Fusion **45** (2003) 1873.
[27] DUX, R., HERRMANN, A., KALLENBACH, A., NEU, R., NEUHAUSER, J., et al., J. Nucl. Mater. **337-339** (2005) 852.
[28] MAYER, M., Carbon and deuterium deposition in the ASDEX Upgrade divertor from 2002–2006, To be published, 2007.
[29] COAD, J., ANDREW, P., HOLE, D., LIKONEN, J., MAYER, M., et al., J. Nucl. Mater. **363-365** (2007) 287.
[30] ANDREW, P., BRENNAN, D., COAD, J., EHRENBERG, J., GADEBERG, M., et al., J. Nucl. Mater. **266-269** (1999) 153.
[31] MERTENS, V., HAAS, G., ROHDE, V., and ASDEX Upgrade Team, Hydrogen gas balance in ASDEX Upgrade with div IIb, in *30th EPS Conference on Controlled Fusion and Plasma Physics*, volume 27A of *europhysics conference abstracts*, pages P–1.128, 2003.
[32] LOARER, T., BROSSET, C., BUCALOSSI, J., COAD, P., ESSER, G., et al., Gas balance and fuel retention in fusion devices, in *Proceedings of the 21st Fusion Energy Conference*, page EX/P3.6, IAEA, 2007.
[33] TSITRONE, E., J. Nucl. Mater. **363-365** (2007) 12.
[34] ROTH, J., ALIMOV, V., GOLUBEVA, A., DOERNER, R., TSITRONE, E., et al., J. Nucl. Mater. **363-365** (2007) 822.
[35] MAYER, M., LIKONEN, J., COAD, J., MAIER, H., BALDEN, M., et al., J. Nucl. Mater. **363-365** (2007) 101.
[36] A.KIRSCHNER, BORODIN, D., DROSTE, S., PHILIPPS, V., SAMM, U., et al., J. Nucl. Mater. (2007).
[37] SHIMADA, M., COSTLEY, A., FEDERICI, G., IOKI, K., KUKUSHKIN, A., et al., J. Nucl. Mater. **337-339** (2005) 808.
[38] COUNSELL, G., COAD, P., GRISOLA, C., HOPF, C., JACOB, W., et al., Plasma Phys. Controlled Fusion **48** (2006) B189.